Supplemental Figures to "Berry monopole-induced nonlinear Hall effect in a chiral Weyl semimetal"

Table of content

Optical and scanning electron microscopy image of the sample

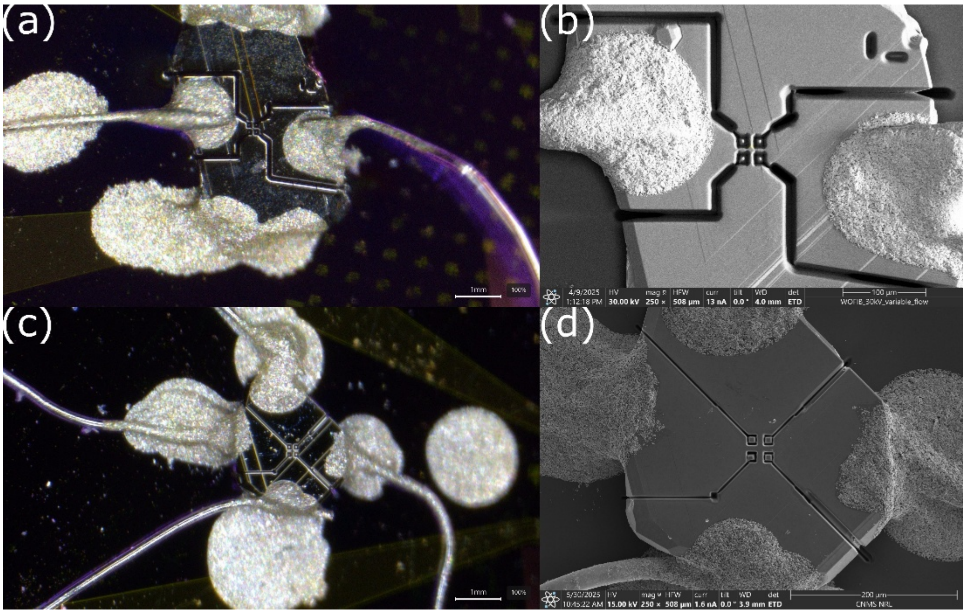

Figure S1 The optical (a, c) and electron (b, d) images of the CoSi sample measured in this work. Sample one is shown by panel (a, b), and Sample two is shown by panel (c, d).

Tensor analysis for the nonlinear Hall conductivity in the [111] plane

An orthogonal coordinate set writes,

$$x = \frac{x_o - y_o}{\sqrt{2}}, y = \frac{x_o + y_o - 2z_o}{\sqrt{6}}, z = \frac{x_o + y_o + z_o}{\sqrt{3}}$$

Here, $x_o/y_o/z_o$ are the original Cartesian axes, and x/y are the new axes in the [111] plane, which form an orthogonal basis with z.

In this experiment, we need to include an additional transformation matrix for a rotation centering around the 111-axis by θ degrees, which writes,

$$x' = \cos\theta\, x + sin\theta\, y, y' = -sin\theta\, x + cos\theta\, y, z' = z$$

The coordinate transformation is shown in Figure S2.

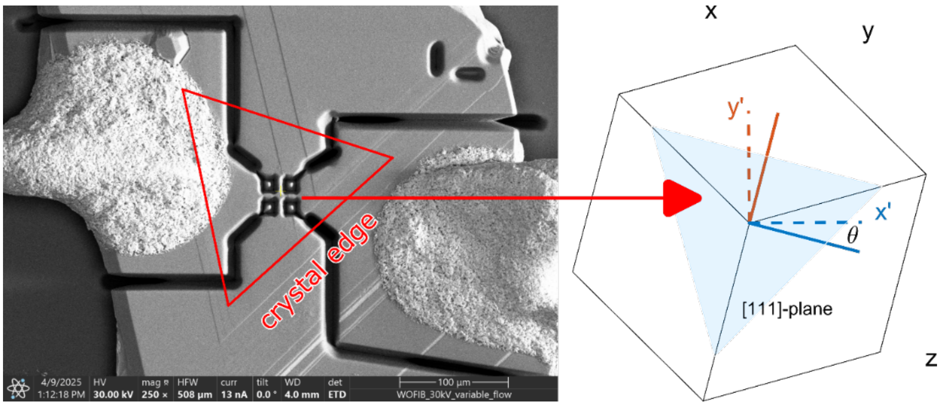

Figure S2 The scanning electron microscope image of the CoSi sample reveals step edges forming a triangular pattern, characteristic of the [111] crystal facet, as shown in the figure on the right.

The total transformation matrix is then given by,

$$U = \begin{pmatrix} \frac{\sin\theta}{\sqrt{6}} + \frac{\cos\theta}{\sqrt{2}} & \frac{\sin\theta}{\sqrt{6}} - \frac{\cos\theta}{\sqrt{2}} & -\frac{2\sin\theta}{\sqrt{6}} \\ \frac{\cos\theta}{\sqrt{6}} - \frac{\sin\theta}{\sqrt{2}} & \frac{\cos\theta}{\sqrt{6}} + \frac{\sin\theta}{\sqrt{2}} & -\frac{2\cos\theta}{\sqrt{6}} \\ \frac{1}{\sqrt{3}} & \frac{1}{\sqrt{3}} & \frac{1}{\sqrt{3}} \end{pmatrix}$$

The cubic structure of the crystal ensures that,

$$\chi_{xyz} = \chi_{permutation\{x,y,z\}} = \chi$$

Then, the measured signal in the experimental setting is given by,

$$\chi_{y'y'x'} = -\frac{2sin3\theta}{\sqrt{6}}\chi_{xyz}$$

Plugging in the experimental value of $\theta = 14.8 \approx 15$ degree, we have $\chi_{y'y'x'} = -\chi_{xyz}/\sqrt{3}$.

Carrier concentration and mobility from Hall effect measurement

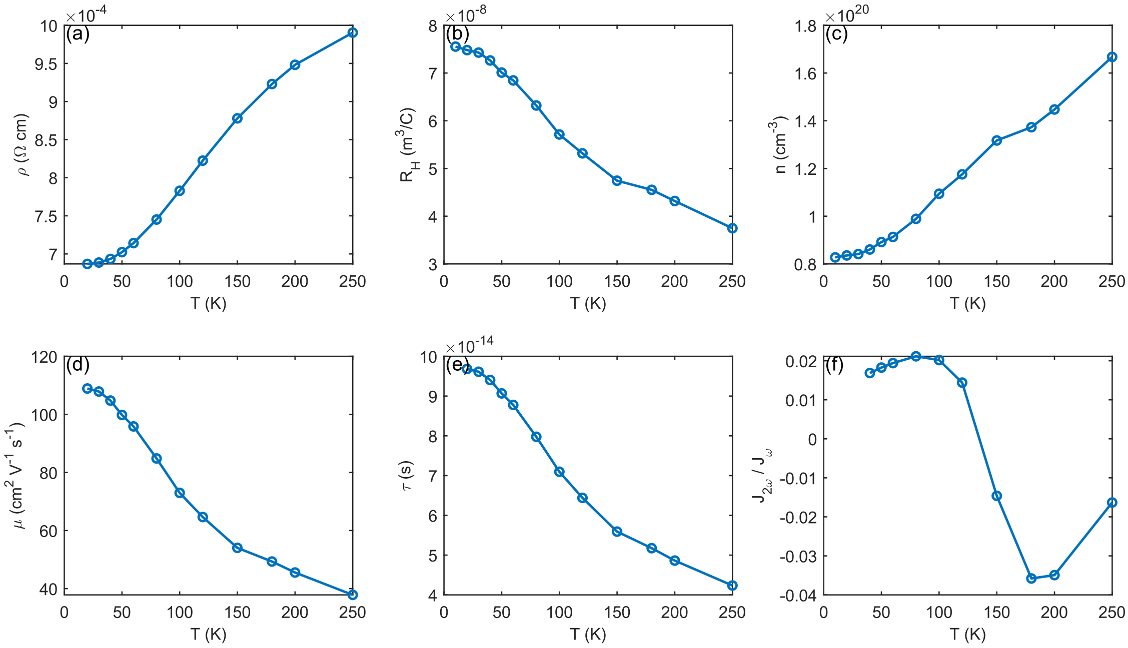

Figure S3 The electrical properties of CoSi sample-I. (a) resistivity, (b) Hall coefficient (c) carrier concentration and (d) carrier mobility. The electron relaxation time (e) is estimated by $\tau = \frac{\hbar(3\pi^2)^{1/3}}{v_F e^2}\frac{1}{\rho n^{2/3}}$, and the nonlinear current – Drude current ratio (f) is calculated by $J_{2\omega}/J_\omega = \chi\rho^2 J_\omega$ at $J_\omega = 1\ mA\ \mu m^{-2}$.

Frequency dependence of the second order voltage-current relation

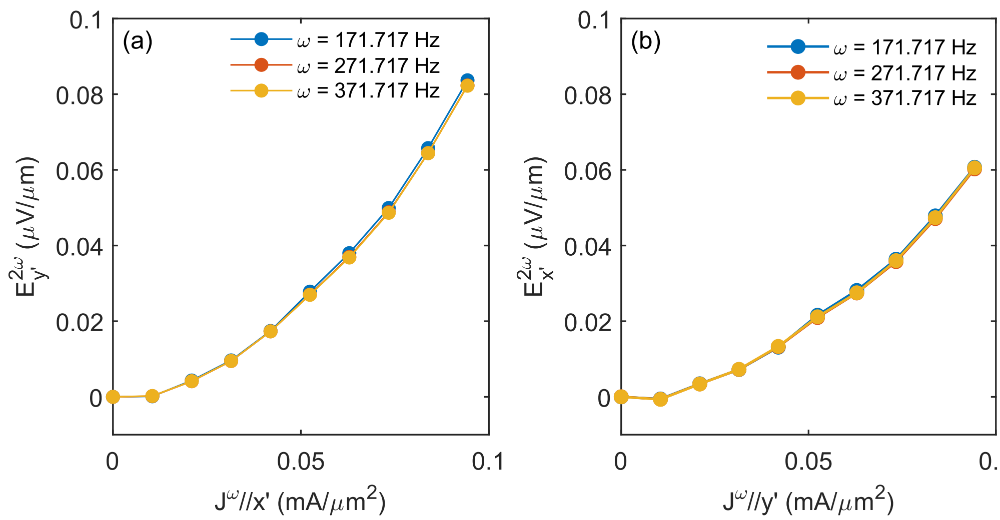

Figure S4 Frequency dependence of the quadratic $E^{2\omega} - J^{\omega}$ relation. At T = 120.0 K and B = 9.0 T, the transverse second harmonic voltage in response to electric currents along the x'-directions and y'-directions were measured. For excitation frequency at 171.717, 271.717 and 371.717 Hz, the $E^{2\omega} - J^{\omega}$ relation is quadratic, and clearly frequency independent.

Symmetric and asymmetric components of the nonlinear Hall conductivity

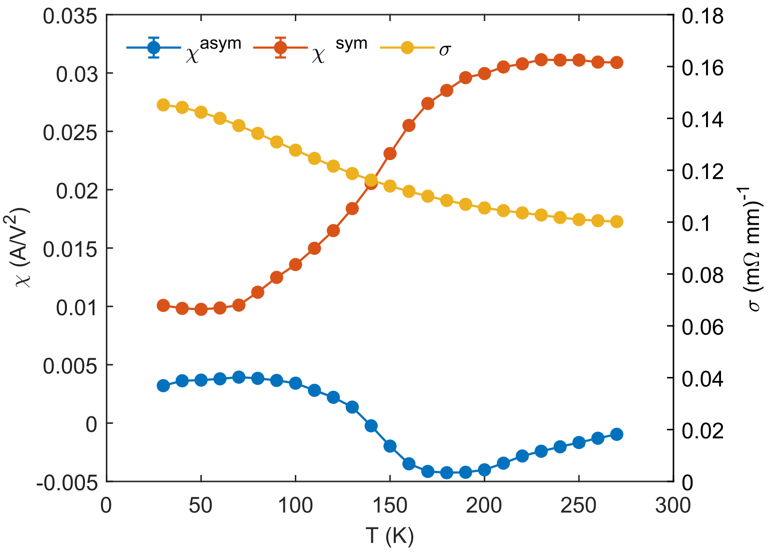

Figure S5 The symmetric and anti-symmetric components of the nonlinear Hall conductivity for sample 1. The right panel also shows the electric conductivity of this sample.

Voltage-current relation asymmetric field induced changes in second harmonic voltage

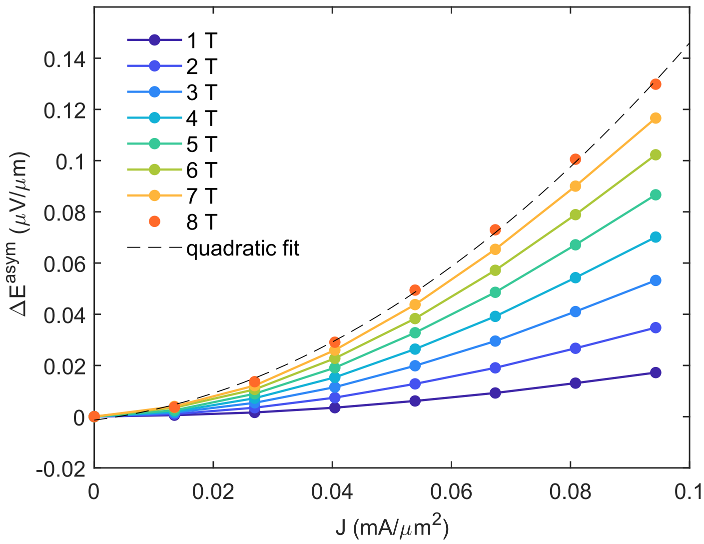

Figure S6 The drive-response relation for the asymmetric field induced changes in second harmonic voltage response. The measurement is conducted at T = 10.0 K where the field effect is most prominent. The $E - J$ still clearly follows a quadratic relation.